Geochemistry Geophysics Geosystems G3

*Article*
Volume 12, Number 7
12 July 2011
Q07006, doi:10.1029/2011GC003501
ISSN: 1525-2027

Published by AGU and the Geochemical Society

# Modeling sulfate reduction in methane hydrate-bearing continental margin sediments: Does a sulfate-methane transition require anaerobic oxidation of methane?

**A. Malinverno**

*Lamont-Doherty Earth Observatory, Earth Institute at Columbia University, 61 Route 9W, Palisades, New York 10964, USA (alberto@ldeo.columbia.edu)*

**J. W. Pohlman**

*Woods Hole Coastal and Marine Science Center, U.S. Geological Survey, 384 Woods Hole Road, Woods Hole, Massachusetts 02543, USA*

[1] The sulfate-methane transition (SMT), a biogeochemical zone where sulfate and methane are metabolized, is commonly observed at shallow depths (1–30 mbsf) in methane-bearing marine sediments. Two processes consume sulfate at and above the SMT, anaerobic oxidation of methane (AOM) and organoclastic sulfate reduction (OSR). Differentiating the relative contribution of each process is critical to estimate methane flux into the SMT, which, in turn, is necessary to predict deeper occurrences of gas hydrates in continental margin sediments. To evaluate the relative importance of these two sulfate reduction pathways, we developed a diagenetic model to compute the pore water concentrations of sulfate, methane, and dissolved inorganic carbon (DIC). By separately tracking DIC containing $^{12}C$ and $^{13}C$, the model also computes $\delta^{13}C$-DIC values. The model reproduces common observations from methane-rich sediments: a well-defined SMT with no methane above and no sulfate below and a $\delta^{13}C$-DIC minimum at the SMT. The model also highlights the role of upward diffusing $^{13}C$-enriched DIC in contributing to the carbon isotope mass balance of DIC. A combination of OSR and AOM, each consuming similar amounts of sulfate, matches observations from Site U1325 (Integrated Ocean Drilling Program Expedition 311, northern Cascadia margin). Without AOM, methane diffuses above the SMT, which contradicts existing field data. The modeling results are generalized with a dimensional analysis to the range of SMT depths and sedimentation rates typical of continental margins. The modeling shows that AOM must be active to establish an SMT wherein methane is quantitatively consumed and the $\delta^{13}C$-DIC minimum occurs. The presence of an SMT generally requires active AOM.

**Components:** 10,900 words, 10 figures, 2 tables.

**Keywords:** anaerobic oxidation of methane; reaction-transport modeling; sulfate reduction.

**Index Terms:** 1009 Geochemistry: Geochemical modeling (3610, 8410); 1051 Geochemistry: Sedimentary geochemistry; 3004 Marine Geology and Geophysics: Gas and hydrate systems.

**Received** 4 January 2011; **Revised** 18 May 2011; **Accepted** 25 May 2011; **Published** 12 July 2011.

Malinverno, A., and J. W. Pohlman (2011), Modeling sulfate reduction in methane hydrate-bearing continental margin sediments: Does a sulfate-methane transition require anaerobic oxidation of methane?, *Geochem. Geophys. Geosyst.*, *12*, Q07006, doi:10.1029/2011GC003501.

## 1. Introduction

[2] Methane-bearing continental margin sediments have characteristic near-seafloor geochemical profiles, schematically illustrated in Figure 1 [e.g., *Claypool and Threlkeld*, 1983; *Borowski et al.*, 1996, 2000; *Burns*, 1998; *Moore et al.*, 2004; *Treude et al.*, 2005; *Claypool et al.*, 2006; *Sivan et al.*, 2007; *Snyder et al.*, 2007; *Kastner et al.*, 2008a; *Pohlman et al.*, 2008; *Ussler and Paull*, 2008]. These profiles are strongly influenced by microbially mediated sulfate reduction processes that oxidize methane and more complex organic compounds to carbon dioxide. Anaerobic oxidation of methane (AOM) couples sulfate reduction to methane oxidation by the net reaction [*Reeburgh*, 1976; *Hoehler et al.*, 1994; *Hinrichs and Boetius*, 2002]

$$SO_4^{2-} + CH_4 \rightarrow HS^- + HCO_3^- + H_2O \quad (1)$$

and occurs at the sulfate-methane transition (SMT) where seawater sulfate encounters methane migrating from below (acronyms used in this paper are listed in Table 1). Organoclastic sulfate reduction (OSR) occurs in the sulfate reduction zone (SRZ) between the seafloor and the SMT, and couples sulfate reduction to the oxidation of complex organic molecules by the generalized reaction [*Claypool and Kaplan*, 1974; *Berner*, 1980]

$$SO_4^{2-} + 2CH_2O \rightarrow H_2S + 2HCO_3^-. \quad (2)$$

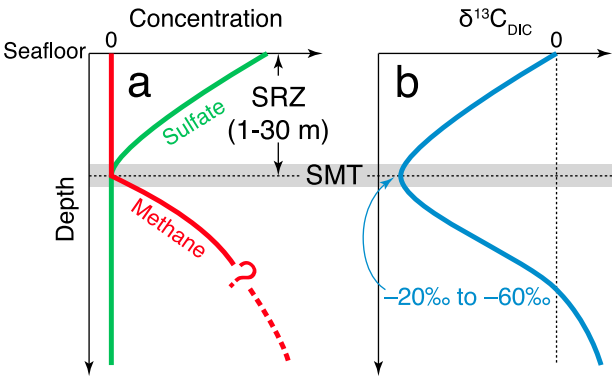


**Figure 1.** Typical near-seafloor geochemical profiles observed in methane-rich sediment sequences. (a) Sulfate is completely consumed in a sulfate reduction zone (SRZ) with a sulfate-methane transition (SMT) at its base. The methane concentration at depth is difficult to measure because of methane loss in core samples (see the text). (b) A minimum in the $\delta^{13}$C-DIC profile is located at the SMT.

**Table 1.** List of Acronyms Used in This Paper

| Acronym | Definition |
|---|---|
| AOM | anaerobic oxidation of methane |
| DIC | dissolved inorganic carbon |
| OSR | organoclastic sulfate reduction |
| SMT | sulfate-methane transition |
| SRZ | sulfate reduction zone |
| mbsf | meters below seafloor |

[3] When AOM is the only sulfate reduction process, sulfate and methane are consumed in a 1:1 molar ratio (reaction (1)) and the fluxes of sulfate and methane into the SMT must be the same. As the methane flux and associated SMT depth are, in principle, related to the depth of the shallowest gas hydrate occurrence, SMT depths have been suggested as a technique for predicting the presence of gas hydrate in the deeper sedimentary system [*Borowski et al.*, 1996].

[4] Using near-seafloor geochemical observations as surface expressions of underlying gas hydrate occurrences is an intriguing possibility. Collecting and analyzing shallow sediment cores is less costly and complex than obtaining geophysical data or drilling to directly recover gas hydrate. However, complicating factors limit the utility of geochemical data as a prospecting tool for gas hydrate. First, near-seafloor geochemical inferences of deeper gas hydrate are well established in "stratigraphic" or "distributed" gas hydrate systems. In these systems, gas hydrate forms in a broad depth interval within the stability zone and methane transport by diffusion is important [*Milkov and Sassen*, 2002; *Claypool et al.*, 2006; *Tréhu et al.*, 2006]. In "structural" or "focused" systems, where methane transported by fluid flow concentrates gas hydrate near the seafloor [*Torres et al.*, 2004], elevated temperatures or salinity in the pore fluids may disrupt the gas hydrate stability conditions [*Ruppel et al.*, 2005; *Paull et al.*, 2005]. In this study we concentrate on the stratigraphic systems that contain the largest volumes of gas hydrates globally [*Milkov and Sassen*, 2002].

[5] An additional challenge for using geochemical data to estimate methane flux and to infer the occurrence of deeply buried gas hydrate is determining what fraction of the sulfate is consumed by AOM or OSR. Sulfate lost to OSR will lead to an overestimate of the actual methane flux if AOM is assumed to be the only sulfate reduction process. Constraining the relative balance of OSR and AOM is critical for understanding how geochemical data can be used to infer the distribution of gas hydrate in marine sediments [*Borowski et al.*, 1996]

and to quantify the capacity of AOM to mitigate the transfer of the greenhouse gas methane into the oceans and ultimately the atmosphere [*Reeburgh*, 2007].

[6] The general occurrence of AOM in continental margin sediments overlying stratigraphic gas hydrates has been questioned by *Claypool et al.* [2006] and *Kastner et al.* [2008a, 2008b]. These authors propose that the primary sink for sulfate is OSR when the $\delta^{13}$C-DIC minimum at the SMT is less negative than that of DIC produced from methane by AOM, and where the DIC and sulfate concentrations in the SRZ follow a 2:1 stoichiometric relationship (reaction (2)). However, these mass balance arguments may not hold in settings where deep-sourced DIC is fluxing upward into the SMT [*Sivan et al.*, 2007; *Dickens and Snyder*, 2009].

[7] In this study, we apply reaction-transport diagenetic modeling [*Berner*, 1980; *Boudreau*, 1997] to determine the combination of OSR and AOM that matches the basic geochemical observations from a site drilled in the northern Cascadia margin (Integrated Ocean Drilling Program (IODP) Site U1325 [*Riedel et al.*, 2006]). The modeling compares concentration gradients of sulfate and methane to estimate the relative importance of OSR and AOM, as done in previous studies [*Niewöhner et al.*, 1998; *Borowski et al.*, 2000; *Moore et al.*, 2004; *Treude et al.*, 2005; *Snyder et al.*, 2007]. We also compute the concentration and $\delta^{13}$C of DIC to determine how they are affected by the balance of OSR and AOM. The computed DIC concentrations and $\delta^{13}$C values allow us to test whether the observations noted by *Claypool et al.* [2006] and *Kastner et al.* [2008a, 2008b] support OSR being the dominant sulfate-consuming process. We close by discussing the general implications of the modeling results for the occurrence of AOM in methane-bearing continental margin sediments.

## 2. Modeling

[8] The fundamental equation of diagenetic modeling [*Berner*, 1980; *Boudreau*, 1997] expresses local mass balance in the concentration $c$ of a solute:

$$\frac{\partial}{\partial t}(\phi c) = \frac{\partial}{\partial z}\left[D\phi\frac{\partial c}{\partial z}\right] - \frac{\partial}{\partial z}(v\phi c) + \phi\sum_{i=1}^{N} Q_i, \qquad (3)$$

where $\phi$ is porosity, $D$ is the diffusion coefficient in bulk sediment, $v$ is the vertical velocity of the pore fluid, and the reaction terms $Q_i$ define $N$ sources and sinks for the solute. Depth $z$, fluid velocity $v$ and sedimentation rate are all defined with respect to a fixed sediment-water interface.

[9] To obtain an analytic solution of equation (3), we assume steady state conditions (so the time derivative is zero), a constant porosity with depth, and no fluid advection. Constant porosity implies no compaction and, in the absence of fluid advection, a fluid velocity $v$ that equals the sedimentation rate. These assumptions turn equation (3) into an ordinary differential equation that we solve with a Laplace transform method (see Appendix A). This analytic solution is useful because the results are easily reproducible and because it complements the numerical solutions most commonly employed in this kind of modeling [e.g., *Davie and Buffett*, 2001; *Bhatnagar et al.*, 2007; *Sivan et al.*, 2007]. While numerical solutions are more flexible and do not require the assumptions made here, an analytic treatment is adequate for our purpose, which is to quantify the major effects of diffusion, burial, and solute generation or consumption on steady state concentrations and isotopic compositions. In the discussion, we address the sensitivity of the modeling results when some of the assumptions are relaxed (e.g., allowing for pore fluid advection) and when some uncertain parameter values are changed (e.g., the sedimentation rate).

[10] The modeling solves equation (3) to compute steady state concentration profiles of sulfate, methane, and DIC. The concentrations of each solute are calculated separately, but the solutions are coupled by the terms $Q_i$, which account for the depth-dependent reactions that consume and generate solutes. As explained below, the overall reaction rates in the $Q_i$ terms are determined by the need to consume sulfate and methane at the SMT and by methanogenesis driven by organic matter degradation. These overall rates correspond to the product of a reaction time constant by the concentration of the reagents [e.g., *Boudreau*, 1997]. Our treatment gives the same results that would be obtained by using a concentration-based form of the reaction rate while adjusting the reaction time constant to match the pore water chemistry observations.

[11] The equation for sulfate concentration contains two sink terms $Q_i$ that consume sulfate, due to OSR and to AOM. These reactions are assumed to occur at constant rates in two separate depth intervals: within the SRZ for the OSR sink, and in a thin interval about the SMT for the AOM sink. The reaction rate of AOM matches an estimated

diffusive flux of methane into the SMT, obtained from Fick's first law of diffusion given an estimate of the methane concentration gradient immediately below the SMT. The reaction rate of OSR is adjusted to consume all the sulfate that is not consumed by AOM (details of all the reaction terms are in Appendix A).

[12] The equation for methane concentration has two reaction terms: one that consumes methane at the SMT due to AOM and one that accounts for microbial methane generation below the SMT. The reaction term for methane consumption at the SMT due to AOM is the same as that for sulfate consumption, as these solutes are consumed in a 1:1 molar ratio (reaction (1)). The methanogenesis reaction term accounts for microbial methane generation by carbonate reduction coupled with organic matter degradation as in the overall net reaction [*Claypool and Kaplan*, 1974]

$$2CH_2O \rightarrow CH_4 + CO_2. \quad (4)$$

The methanogenesis reaction term starts at the SMT and decreases exponentially with depth, accounting for the progressive consumption of organic matter as sediment is buried. This exponential depth dependence is the solution of a simple equation where the rate of methanogenesis is proportional to a reaction time constant multiplied by the concentration of metabolizable solid organic matter [*Davie and Buffett*, 2001; *Malinverno et al.*, 2008; *Malinverno*, 2010]. The rate of methanogenesis at the SMT is set to match the estimated concentration gradient of methane at the SMT (details are in Appendix A).

[13] We include this methane production term because there is abundant evidence for in situ microbial methanogenesis in gas hydrate-bearing continental margin sediments. Methane is generated in marine sediments beneath the SRZ as part of the normal process of organic matter degradation [*Claypool and Kaplan*, 1974; *Berner*, 1980]. Experiments show that microbes within sediments produce methane, with the highest numbers of methanogens being found near the seafloor [*Colwell et al.*, 2008]. In a transect drilled across the Northern Cascadia margin, *Pohlman et al.* [2009] found that the isotopic compositions of methane and $CO_2$ are consistent with in situ microbial methane generation by carbonate reduction as in reaction (4). The transect studied by *Pohlman et al.* [2009] includes IODP Site U1325, whose geochemical data will be later compared to the modeling results. At Site U1325, *Malinverno* [2010] showed with a reaction-transport model that microbial in situ methane generation was sufficient to account for the observed amounts of gas hydrates. The results of *Malinverno* [2010] will be used here to estimate the methane concentration gradient that constrains the methanogenesis reaction term.

[14] The equation for DIC concentration has three reaction terms that account for DIC produced by OSR, AOM, and organic matter degradation. The reaction rates in these terms are related to those for sulfate and methane as follows. The OSR term generates two units of DIC for each unit of sulfate consumed (reaction (2)), the AOM term generates one unit of DIC for each unit of sulfate consumed (reaction (1)), and the organic matter degradation term produces one unit of DIC for each unit of methane produced (reaction (4)).

[15] To compute a $\delta^{13}$C-DIC profile, the modeling solves two equations for DIC containing $^{12}$C and $^{13}$C. The strengths of the reaction terms in these equations are adjusted to match the $\delta^{13}$C of the DIC generated by different reactions (see Appendix A). Because upward fluxing methane is quantitatively oxidized to $CO_2$, there are no fractionation effects associated with AOM [*Whiticar*, 1999]. Hence, in the modeling the $\delta^{13}$C of the DIC generated by AOM is the same as the $\delta^{13}$C of methane. As OSR does not appreciably fractionate C isotopes [*Blair et al.*, 1994], the $\delta^{13}$C of DIC produced by OSR is assumed to have the same $\delta^{13}$C as $C_{org}$. DIC is also produced below the SMT by organic matter degradation coupled with methanogenesis (reaction (4)). To balance carbon in reaction (4), the $\delta^{13}$C of this DIC must be

$$\delta^{13}\text{C-DIC} = 2\,\delta^{13}\text{C-C}_{org} - \delta^{13}\text{C-CH}_4. \quad (5)$$

[16] The model does not include authigenic carbonate formation, which would decrease the DIC concentration [*Sivan et al.*, 2007; *Snyder et al.*, 2007]. We consider the implications of this assumption in the sensitivity analysis. To ensure that the modeled reactions do not require unrealistic amounts of $C_{org}$ for OSR and organic matter degradation, the modeling also tracks the solid $C_{org}$ content of the bulk sediment.

## 3. IODP Site U1325

[17] To compare modeling predictions to actual observations, we run the model with parameters

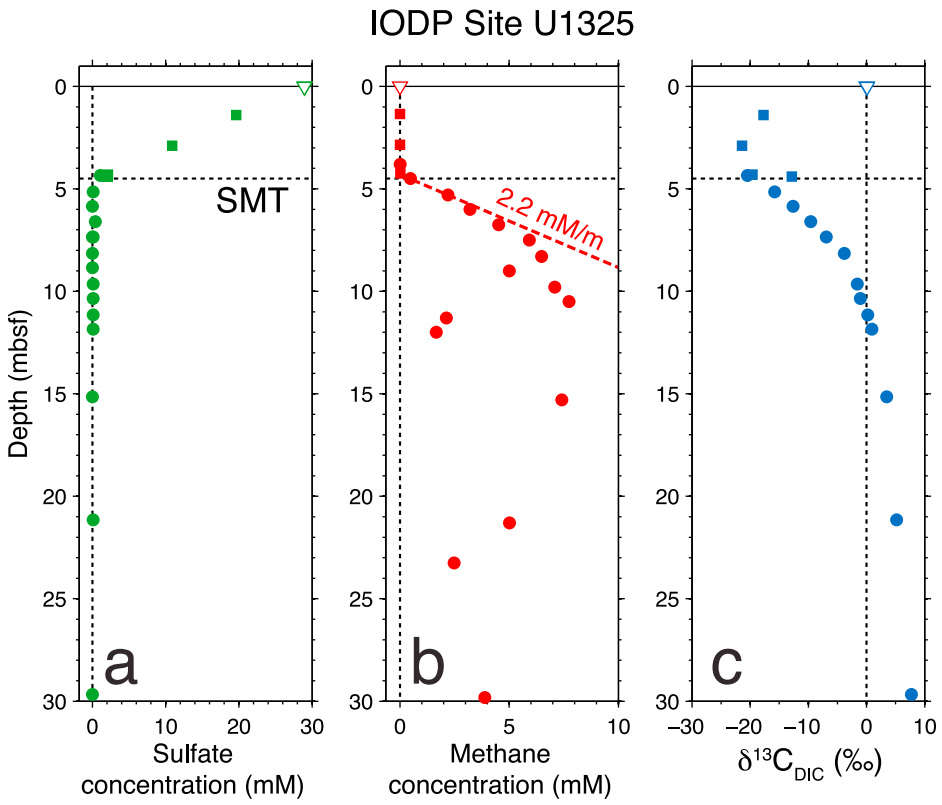


**Figure 2.** Pore water data measured at IODP Site U1325. (a) Sulfate and (b) methane concentrations after *Riedel et al.* [2006] and (c) $\delta^{13}$C-DIC data after *Torres and Kastner* [2009]. Circles are samples from Hole U1325B, squares are from Hole U1325D, and triangles are ocean water values. Sample depths in Hole U1325B were shifted by 3 m to match the SMT observed in Hole U1325D (see the text). The dashed line in Figure 2b indicates the methane concentration gradient determined from the first few measurements below the SMT.

measured and estimated at Site U1325, a site recently drilled on the northern Cascadia margin during Expedition 311 of the Integrated Ocean Drilling Program [*Riedel et al.*, 2006]. Figure 2 shows the pore water data measured in two holes at Site U1325. The observed depth of the SMT was not consistent in these two holes, and the interpretation was that Hole U1325B missed the mudline by about 3 m [see *Riedel et al.*, 2006, U1325 chapter]. To obtain a consistent data set, 3 m were added to the data from Hole U1325B plotted in Figure 2.

[18] Table 2 lists the key Site U1325 parameters used in the modeling. A SMT thickness of 0.5 m is broadly consistent with the transition between the sulfate and methane-bearing intervals observed at Site U1325. The sedimentation rate of 196 m/Ma is from the depth of a diatom event dated at 1 Ma or younger [*Akiba et al.*, 2009]. This is a reasonable average long-term sedimentation rate, but it is not well constrained and could be higher. A shallower diatom event gives a rate twice as large (408 m/Ma) for the top 123 m. Given the uncertainties in the thickness of the SMT and in the sedimentation rate at Site U1325, they will be varied later to examine the sensitivity of the results.

[19] The methane concentration gradient estimated at Site U1325 constrains the rate of AOM and methanogenesis in the modeling. There are several ways to estimate the methane gradient:

[20] 1. Perform a linear interpolation from the SMT, where the methane concentration is effectively zero, to the depth of the shallowest gas hydrate occurrence (73 mbsf at Site U1325 [*Malinverno et al.*, 2008]), where methane concentrations must reach solubility in equilibrium with gas hydrate. Using the solubility curve of *Davie et al.* [2004], this approach gives a gradient of ~1 mM/m. However, methane generation below the SMT results in a concave downward profile [*Schulz*, 2006], and the actual methane gradient at the

**Table 2.** Modeling Parameters (From IODP Site U1325, Northern Cascadia Margin)

| Parameter | Value | Reference |
|---|---|---|
| Depth of SMT | 4.5 mbsf | *Riedel et al.* [2006] |
| Thickness of SMT | 0.5 m | see text |
| Sedimentation rate | 196 m/Ma | *Akiba et al.* [2009] |
| Methane concentration gradient below the SMT | 2.3 mM/m | see text |
| Reaction rate for methanogenesis | $10^{-13}$ $s^{-1}$ | *Malinverno* [2010] |
| $\delta^{13}C_{org}$ | −25‰ | *Kim and Lee* [2009] |
| $\delta^{13}C$-$CH_4$ near the SMT | −80‰ | *Pohlman et al.* [2009] |
| Minimum $\delta^{13}C$-DIC at the SMT | −21.4‰ | *Torres and Kastner* [2009] |
| Dry weight fraction of $C_{org}$ at the seafloor | ~1.5% | *Riedel et al.* [2006] |
| Dry weight fraction of $C_{org}$ at depth | ~0.5% | *Riedel et al.* [2006] |

SMT must be greater than the value obtained by linear interpolation.

[21] 2. Use measured pore water methane concentrations from the SMT to the depth where the concentrations reach the atmospheric solubility of ~2 mM [*Niewöhner et al.*, 1998; *Treude et al.*, 2005]. Whereas core samples with large in situ methane concentrations degas during recovery, the methane concentrations lower than atmospheric solubility measured just below the SMT can be used to establish the local gradient [*Paull and Ussler*, 2001]. The methane gradient estimated with this technique and data from Site U1325 is 2.2 mM/m, and because of degassing this value is expected to be conservatively low.

[22] 3. Modeling the methane concentrations in the depth interval between the SMT and the top of the gas hydrate-bearing interval gives a slightly higher gradient of 2.3 mM/m [*Malinverno*, 2010]. As this reaction-transport model assumes constant porosity and no upward fluid advection, it is also expected to be conservatively low [*Malinverno et al.*, 2008]. Given that the estimated gradients are conservatively low, we use the greatest among them (2.3 mM/m) and will discuss later the implications of a possibly higher gradient.

[23] For methanogenesis, the Site U1325 modeling of *Malinverno* [2010] estimated a reaction time constant of $10^{-13}$ $s^{-1}$ (1/317 ka), comparable to values obtained in similar settings [*Davie and Buffett*, 2001; *Claypool et al.*, 2006]. This reaction time constant and the assumed methane concentration gradient at the SMT constrain the methanogenesis reaction term (see Appendix A).

[24] To set the production rates of DIC containing $^{12}C$ and $^{13}C$, the modeling needs values for the $\delta^{13}C$ of the DIC generated by different reactions. As noted earlier, the $\delta^{13}C$ of the DIC generated by AOM in the modeling is the same as the $\delta^{13}C$ of the methane near the SMT, which is −80‰ at Site U1325 [*Pohlman et al.*, 2009]. The $\delta^{13}C$ of DIC produced by OSR is the same as that of $C_{org}$, which is −25‰ at Site U1325 [*Kim and Lee*, 2009]. The $\delta^{13}C$ of DIC produced below the SMT by organic matter degradation coupled with methanogenesis (reaction (4)) is given by equation (5).

[25] The minimum $\delta^{13}C$-DIC measured at the SMT of Site U1325 is −21.4‰ [*Torres and Kastner*, 2009]. The similarity of this $\delta^{13}C$-DIC value to the $\delta^{13}C$ of the bulk organic matter is consistent with situations where DIC is a product of OSR [*Presley and Kaplan*, 1968; *McCorkle and Emerson*, 1988; *Blair et al.*, 1994]. As noted earlier, some authors propose that AOM is not active when the minimum $\delta^{13}C$-DIC at the SMT is close to the $\delta^{13}C$ of sediment organic matter [*Claypool et al.*, 2006; *Kastner et al.*, 2008a; *Torres and Kastner*, 2009]. The modeling in this paper will address this question.

[26] Finally, the organic carbon content in the sediment constrains the amount of organic matter available for OSR and organic matter degradation. At Site U1325, $C_{org}$ is ~1.5 wt % at the seafloor and decreases to ~0.5 wt % at depth [*Riedel et al.*, 2006]. The deep $C_{org}$ content is usually assumed to represent refractory organic matter not available for microbially mediated reactions [e.g., *Ingall and Van Cappellen*, 1990]. Thus, the diagenetic reactions modeled here are limited to using about 1 wt % $C_{org}$. The modeling computes a total $C_{org}$ content curve by adding the amount consumed by the modeled reactions to the deep value of 0.5 wt % observed at Site U1325. This calculation neglects the fraction of organic matter that goes into acetate and other dissolved organic compounds [*Heuer et al.*, 2009].

## 4. Modeling Results

[27] We consider the results for three scenarios: (1) Only AOM consumes sulfate, (2) only OSR

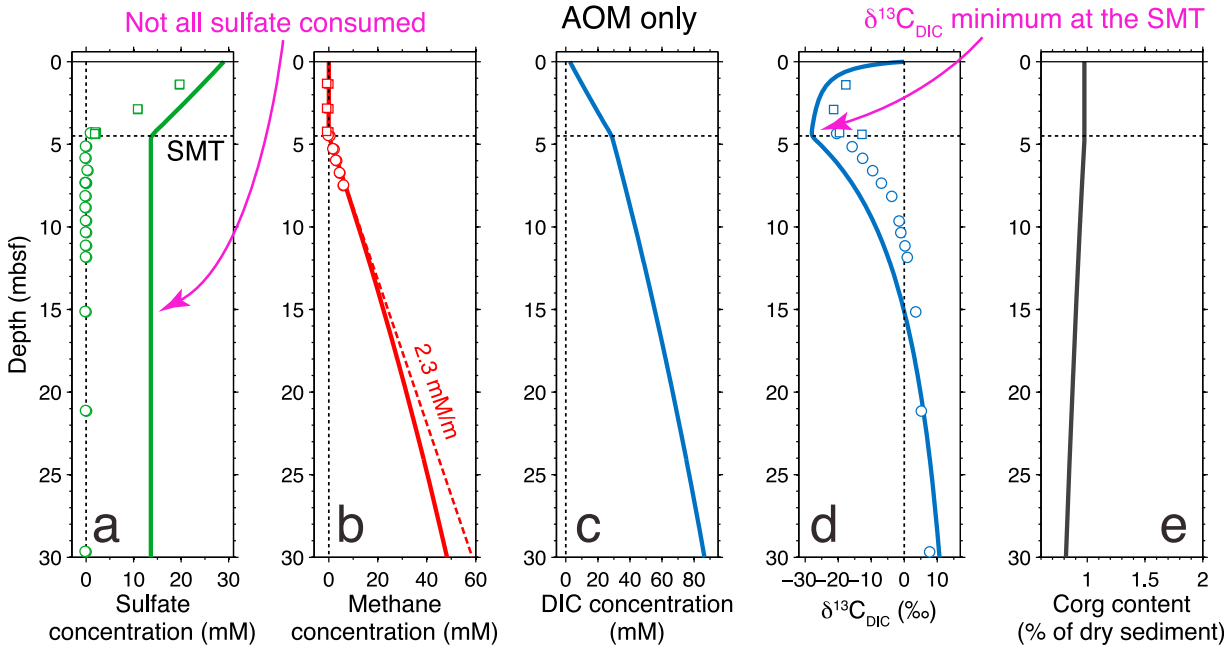


**Figure 3.** Modeled profiles of (a–c) solute concentrations, (d) $\delta^{13}$C-DIC, and (e) $C_{org}$ content if anaerobic oxidation of methane (AOM) is the only sulfate-consuming reaction at Site U1325. The estimated methane concentration gradient (2.3 mM/m at the SMT) in Figure 3b is only enough to result in the consumption of half of the sulfate. The minimum $\delta^{13}$C-DIC in Figure 3d is centered on the SMT. Circles and squares in Figures 3a, 3b, and 3d are data from Hole U1325B and Hole U1325D, respectively (see Figure 2).

consumes sulfate, and (3) both AOM and OSR consume sulfate.

## 4.1. Only AOM Consumes Sulfate

[28] In this scenario, methane is oxidized by AOM over a 0.5 m thick SMT, and the methane oxidation rate is adjusted to consume all the methane that fluxes upward for the concentration gradient estimated at Site U1325 (see Appendix A). No sulfate is consumed by OSR in this scenario, and the reaction rates for OSR are set to zero.

[29] The results, illustrated in Figure 3, show that AOM driven by the estimated methane concentration gradient consumes 53% of the total sulfate, and the presence of sulfate below the SMT contradicts the observations. If the estimated methane gradient is accurate, AOM cannot be the only sulfate-consuming reaction at Site U1325. A methane gradient about twice that estimated for Site U1325 is necessary for AOM to completely consume the sulfate. The effect of a higher methane gradient will be discussed later.

[30] The modeled $\delta^{13}$C-DIC displays a −28‰ minimum at the SMT, where $^{13}$C-depleted DIC is generated by AOM. This minimum value is considerably less negative than the $\delta^{13}$C of the DIC produced by AOM from methane (−80‰) because $^{13}$C-enriched DIC generated from organic matter degradation diffuses upward into the SMT [*Sivan et al.*, 2007; *Dickens and Snyder*, 2009]. The modeled value is slightly more negative than the value measured at Site U1325. Figure 3e also shows the modeled $C_{org}$ content of the sediment. Without OSR, organic matter is only consumed below the SRZ (reaction (4)) and the required amount of $C_{org}$ at the seafloor is only ~1%.

[31] When AOM is the dominant reaction, *Claypool et al.* [2006] and *Kastner et al.* [2008a, 2008b] suggest that the DIC produced and the sulfate consumed in pore water profiles should follow a 1:1 relationship, consistent with the stoichiometry of reaction (1). In the AOM only modeling scenario, however, the computed concentrations of DIC and sulfate in the SRZ follow more closely the 2:1 ratio (Figure 4) expected for OSR (reaction (2)). The reason for this apparent inconsistency is that DIC produced by organic matter degradation diffuses into the SRZ from below [*Dickens and Snyder*, 2009]. This additional DIC increases the DIC-sulfate concentration ratio above the expected 1:1 value for AOM in a closed system.

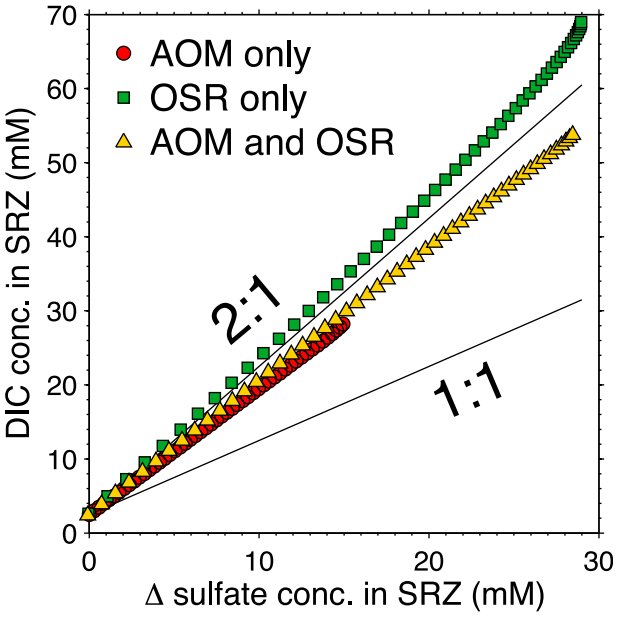


**Figure 4.** Computed DIC-sulfate ratio in the SRZ for three modeling scenarios. The horizontal coordinate is the computed sulfate concentration minus the value at the seafloor (29 mM). Because of DIC diffusing into the SRZ from below, the DIC-sulfate ratio is near 2:1 regardless of the reactions that consume sulfate.

### 4.2. Only OSR Consumes Sulfate

[32] In this scenario, OSR reduces sulfate throughout the SRZ at a constant rate adjusted to consume all the sulfate in the sediment (see Appendix A). The reaction rates for AOM are set to zero.

[33] The modeling results (Figure 5) show concentrations of methane above zero in the SRZ. In the absence of a methane sink at the SMT, methane diffuses into the SRZ and its concentration goes to zero only at the seafloor. The $\delta^{13}$C-DIC minimum is −17.5‰, which is slightly less negative than the value observed at Site U1325, but it is located near the center of the SRZ where $^{13}$C-depleted DIC is generated by OSR. The presence of methane in the SRZ and the location of the $\delta^{13}$C-DIC minimum well above the SMT contradict the observations at Site U1325. OSR cannot be the only sulfate-consuming reaction if methane fluxes upward into the SRZ.

[34] If OSR is the only reaction consuming sulfate, a relatively large amount of $C_{org}$ is required at the seafloor (almost 2%). A comparison of the concentrations of DIC and sulfate in the SRZ (Figure 4) shows a relationship just above the 2:1 line, again because of DIC diffusing into the SRZ from below.

### 4.3. Both AOM and OSR Consume Sulfate

[35] The above modeling scenarios where AOM and OSR are the only sulfate-consuming reactions fundamentally contradict the observed sulfate, methane and DIC isotopic signatures from Site U1325. We consider now their combination. In this scenario, the AOM reaction rate is adjusted to consume all the methane that diffuses into the SMT due to the estimated methane concentration gradient at Site U1325. The rate of sulfate consumption due to OSR (assumed constant throughout the SRZ) is adjusted so that sulfate concentration is zero at the SMT.

[36] This AOM-OSR combination results in a well-defined SMT with no methane above and no sulfate below (Figure 6). The $\delta^{13}$C-DIC curve shows a minimum at the SMT of −26.6‰, close to the value obtained for AOM only and slightly more negative than that observed at Site U1325. The amount of $C_{org}$ required (~1.5% at the seafloor) is consistent with that observed at Site U1325. A comparison of the concentrations of DIC and sulfate in the SRZ (Figure 4) shows a relationship just below the 2:1 line that lies between the AOM-only and OSR-only scenarios.

## 5. Discussion

[37] To summarize, a combination of AOM and OSR is necessary to reproduce the key observations made at Site U1325: a well-defined SMT, with no sulfate below and no methane above, and a $\delta^{13}$C-DIC minimum centered at the SMT. OSR is needed because the estimated methane flux is insufficient to consume all sulfate, and AOM is necessary to oxidize methane at the SMT. If AOM were not active, methane would diffuse upward, contradicting the observed lack of methane above the SMT.

[38] Our analytical model also shows that observations cited in support of OSR being the dominant sulfate-reducing mechanism [*Claypool et al.*, 2006; *Kastner et al.*, 2008a; *Torres and Kastner*, 2009] are not necessarily diagnostic. Regardless of the dominant sulfate-reducing reaction, the modeled minimum in the $\delta^{13}$C-DIC curve at Site U1325 is much less negative than that of the DIC produced by AOM and the DIC-sulfate ratio in the SRZ is nearly 2:1. The reason is diffusion into the SMT of $^{13}$C-enriched DIC that was generated by organic matter degradation below the SRZ [*Sivan et al.*, 2007; *Dickens and Snyder*, 2009]. This diffusion process changes the values of the minimum $\delta^{13}$C-DIC and of the DIC-sulfate ratio from those that would be expected in a closed system.

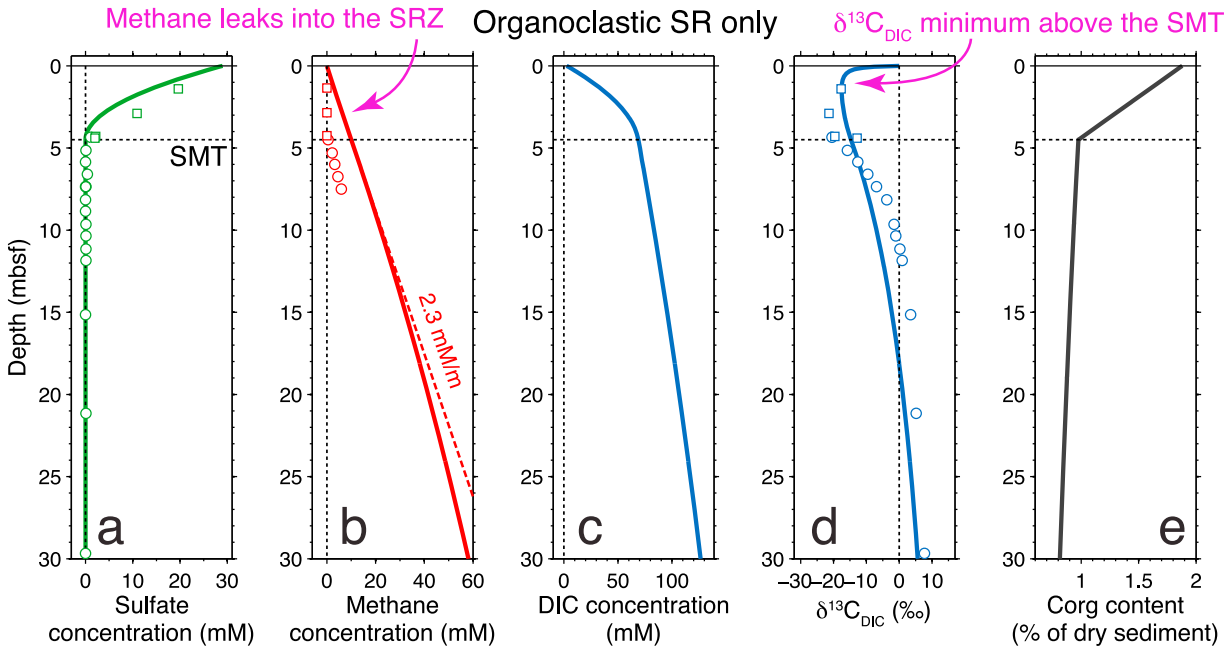


**Figure 5.** Modeled profiles of (a–c) solute concentrations, (d) $\delta^{13}$C-DIC, and (e) $C_{org}$ content if organoclastic sulfate reduction (OSR) is the only sulfate-consuming reaction at Site U1325. As there is no sink for methane due to AOM, methane leaks into the SRZ (Figure 5b). The minimum $\delta^{13}$C-DIC in Figure 5d is well above the SMT. Circles and squares in Figures 5a, 5b, and 5d are data from Hole U1325B and Hole U1325D, respectively (see Figure 2).

[39] These results depend on the modeling assumptions and parameters estimated at Site U1325. Assumptions made to obtain an analytic solution of equation (3) should not significantly affect our results, because very similar results were obtained with numerical simulations of sulfate reduction processes [*Chatterjee et al.*, 2009]. For the remainder of this discussion, we first test the robustness of our results by varying some of the parameters that have a significant uncertainty. We then extend our analysis beyond Site U1325 by exploring whether the widespread observation of a SMT over methane-bearing sediments generally requires active AOM.

## 5.1. Sensitivity Analysis, Site U1325

[40] We carry out this analysis by changing parameters one at a time in the combined AOM-OSR base case that best reproduces the key observations at Site U1325 (Figure 6). The goal is to check whether these parameter changes significantly affect the modeled sulfate and methane concentrations and the character of the $\delta^{13}$C-DIC curve.

### 5.1.1. Fluid Advection

[41] The modeling assumes constant porosity. However, in a compacting sequence, porosity decreases with depth, which drives the pore fluids upward, thereby causing the burial velocity of the pore fluid to be less than the sediment burial rate [*Berner*, 1980]. Also, in accretionary margins, sediment dewatering can result in upward advection that decreases further the fluid burial velocity [e.g., *Bekins and Dreiss*, 1992]. We approximate the effect of fluid advection from compaction and dewatering by setting the fluid burial velocity to less than the sedimentation rate at all depths. In a compacting sequence with a porosity-depth relationship like that at Site U1325, the fluid velocity to sedimentation rate ratio at the sediment-water interface is 0.36. As depth increases, this ratio decreases until the fluid and solid velocities converge to a single value [*Berner*, 1980]. A fluid burial velocity that is 0.36 times the sedimentation rate has a minimal effect on the modeled sulfate and methane concentrations and on the position and value of the $\delta^{13}$C-DIC minimum. The modeling results are visually indistinguishable from those in Figure 6 (actual results not shown).

### 5.1.2. Sedimentation Rate

[42] The sedimentation rate of 196 m/Ma at Site U1325 that we use in the model may be low. When the sedimentation rate is doubled, approximating

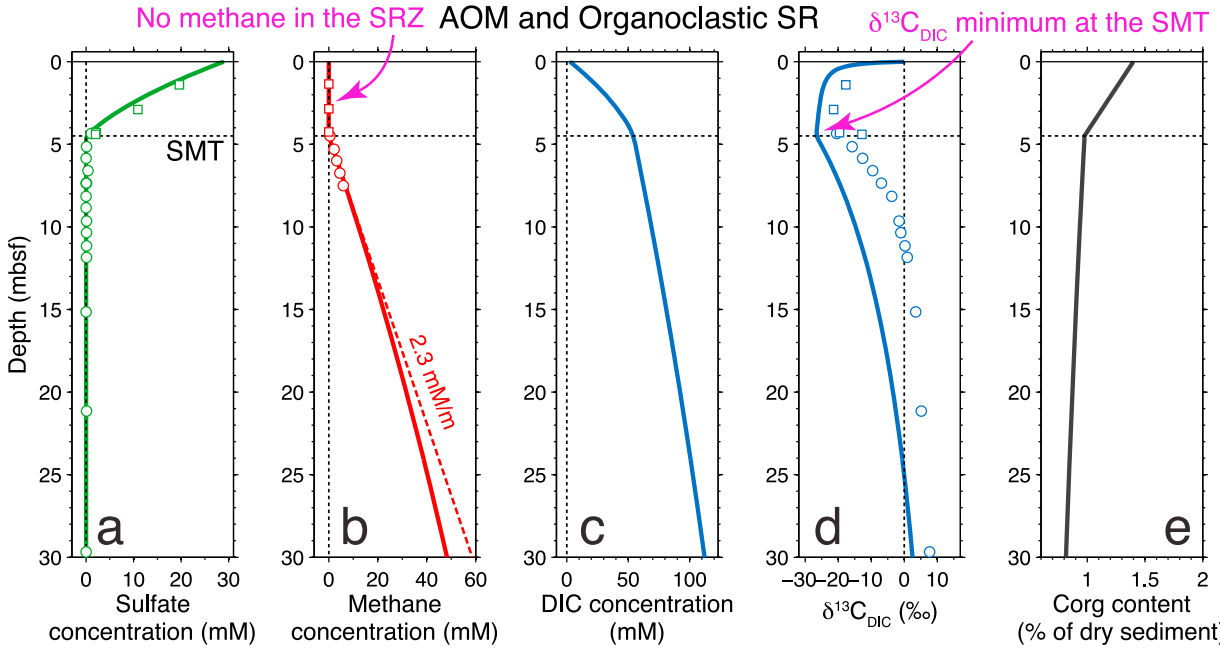


**Figure 6.** Modeled profiles of (a–c) solute concentrations, (d) $\delta^{13}$C-DIC, and (e) $C_{org}$ content if both anaerobic oxidation of methane (AOM) and organoclastic sulfate reduction (OSR) consume sulfate at Site U1325. All sulfate is consumed in the SRZ (Figure 6a) and there is no methane in the SRZ (Figure 6b). The minimum $\delta^{13}$C-DIC in Figure 6d is centered on the SMT. Circles and squares in Figures 6a, 6b, and 6d are data from Hole U1325B and Hole U1325D, respectively (see Figure 2).

the 408 m/Ma estimated for the top 123 m of Site U1325 by *Akiba et al.* [2009], the modeling results are not significantly affected and remain similar to those in Figure 6 (actual results not shown).

### 5.1.3. Thickness of the SMT

[43] The modeling assumed a 0.5 m thick SMT, and varying the SMT thickness between 0.1 and 3 m has no appreciable effect on the results (actual results not shown).

### 5.1.4. Depth of the SMT

[44] We ran the model with a 2 mbsf SMT, which is significantly shallower than the 4.5 mbsf SMT at Site U1325. In this sensitivity analysis, we changed only the depth of the SMT while leaving all other parameters unchanged. Hence, this shallow SMT case does not correspond to a higher methane gradient. The methane gradient, which was not estimated from the SMT depth at Site U1325, was kept at the base case value of 2.3 mM/m. The effects of a higher methane gradient will be explored later in this section.

[45] The modeling results for this shallow SMT are in Figure 7. A combination of AOM and OSR still fits the key observations at Site U1325, and a 2 m deep SMT has little effect on the computed minimum $\delta^{13}$C-DIC (−25‰ instead of −26.5‰). A shallower SMT for a fixed methane gradient requires an increase in the OSR rate to consume all sulfate in a thinner SRZ. This is reflected in a required amount of $C_{org}$ at the seafloor of ~2.5% (Figure 7e), which is higher than that measured at Site U1325. If the SMT is shallower, AOM consumes a smaller fraction of the total sulfate (24%), but it is still important. If the modeling is done without AOM for a 2 mbsf SMT, methane leaks into the SRZ and the minimum $\delta^{13}$C-DIC is located within the SRZ.

### 5.1.5. Higher Rates of OSR Near the Seafloor

[46] For OSR, the modeling assumes a constant sulfate sink throughout the SRZ. The rates of OSR, however, may be highest near the sediment-water interface and decrease with depth in the SRZ [e.g., *Jørgensen et al.*, 2001]. We investigated the effect of this variation with depth by letting the sulfate

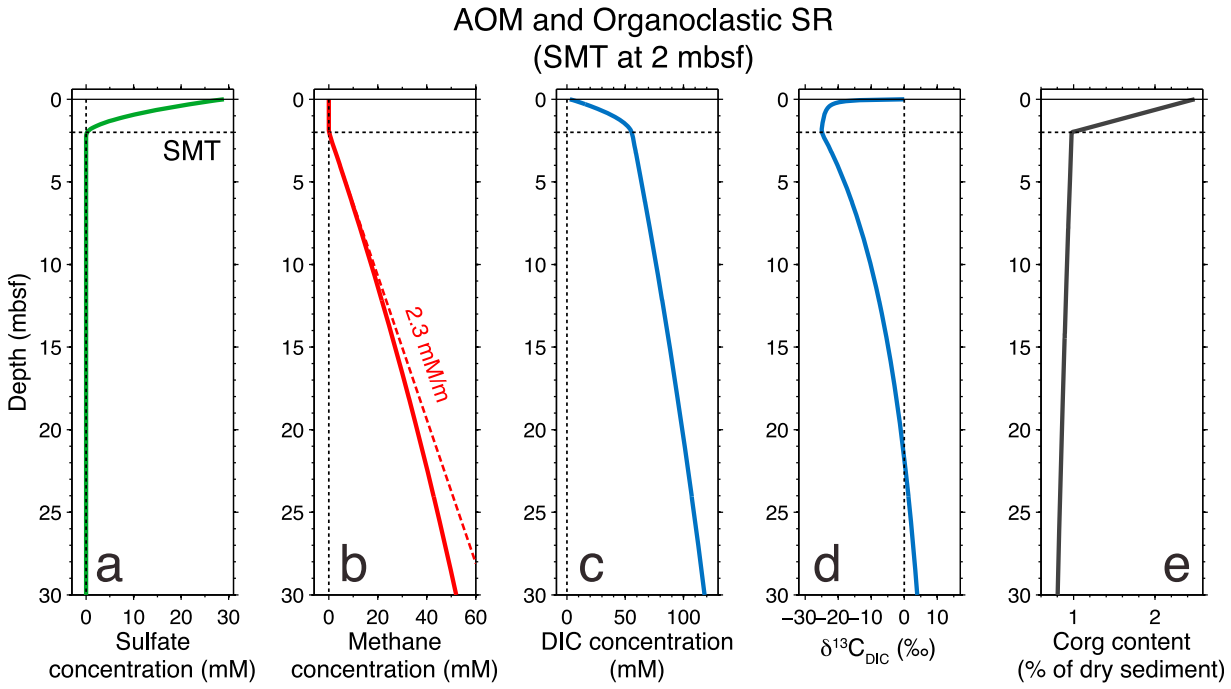


**Figure 7.** Modeled profiles of (a–c) solute concentrations, (d) $\delta^{13}$C-DIC, and (e) $C_{org}$ content if both anaerobic oxidation of methane (AOM) and organoclastic sulfate reduction (OSR) consume sulfate at Site U1325. All model parameters are as in Figure 6 except that the SMT depth is 2 mbsf.

sink rate due to OSR decrease exponentially with depth with a decay constant of 1 m. This means that most of the OSR sulfate sink is near the seafloor (86% in the top 2 m of the SRZ). The only effects of having OSR most active near the sediment-water interface are a slight downward concavity in the modeled sulfate profile and higher overall reaction rates compared to the constant sink (actual results not shown). Near the seafloor, sulfate can more easily diffuse from the ocean reservoir into the sediment and hence higher reaction rates are needed to consume a set amount of sulfate [*Jørgensen et al.*, 2001].

### 5.1.6. Authigenic Carbonate Formation

[47] The modeling does not account for authigenic carbonate formation. Authigenic carbonate formation will not affect the sulfate and methane concentrations and does not fractionate carbon isotopes [*Teichert et al.*, 2005]. Authigenic carbonate formation, however, may decrease the DIC concentration in the sediment column [*Sivan et al.*, 2007] and reduce the upward diffusive flux of DIC into the SMT [*Snyder et al.*, 2007], changing the $\delta^{13}$C-DIC profile. At Site U1325 there is clear evidence of upward DIC flux, as shown by an increase in measured alkalinity (a proxy for DIC [*Claypool et al.*, 2006]) that reaches a maximum well below the SMT at about 30 mbsf [*Riedel et al.*, 2006].

[48] We crudely simulate authigenic carbonate formation in our model by turning off the DIC source below 30 mbsf. This results in a smaller DIC gradient below the SMT and a DIC concentration profile that reaches a constant value below 30 mbsf. The modeled $\delta^{13}$C-DIC curve still has a −31.4‰ minimum at the SMT that is more negative than in the base case of Figure 6 (actual results not shown). The lack of a DIC source at depth, however, gives a $\delta^{13}$C-DIC curve that remains negative everywhere and never reaches the deep +10‰ value observed at Site U1325 [*Torres and Kastner*, 2009]. A mass balance model with a depth-dependent DIC sink for authigenic carbonate formation would be required to properly model the $\delta^{13}$C-DIC profile [e.g., *Moore et al.*, 2004; *Sivan et al.*, 2007]. The depth distribution of authigenic carbonate formation is not well known and determining it is beyond the scope of this work.

[49] We recognize that the results presented here are distinct from cases where the DIC concentration below the SMT does not increase so that there is no upward DIC flux [e.g., *Kastner et al.*, 2008b; *Pohlman et al.*, 2008; *Ussler and Paull*, 2008]. Without an upward DIC flux into the SMT, the $\delta^{13}$C-DIC minimum observed at the SMT is very

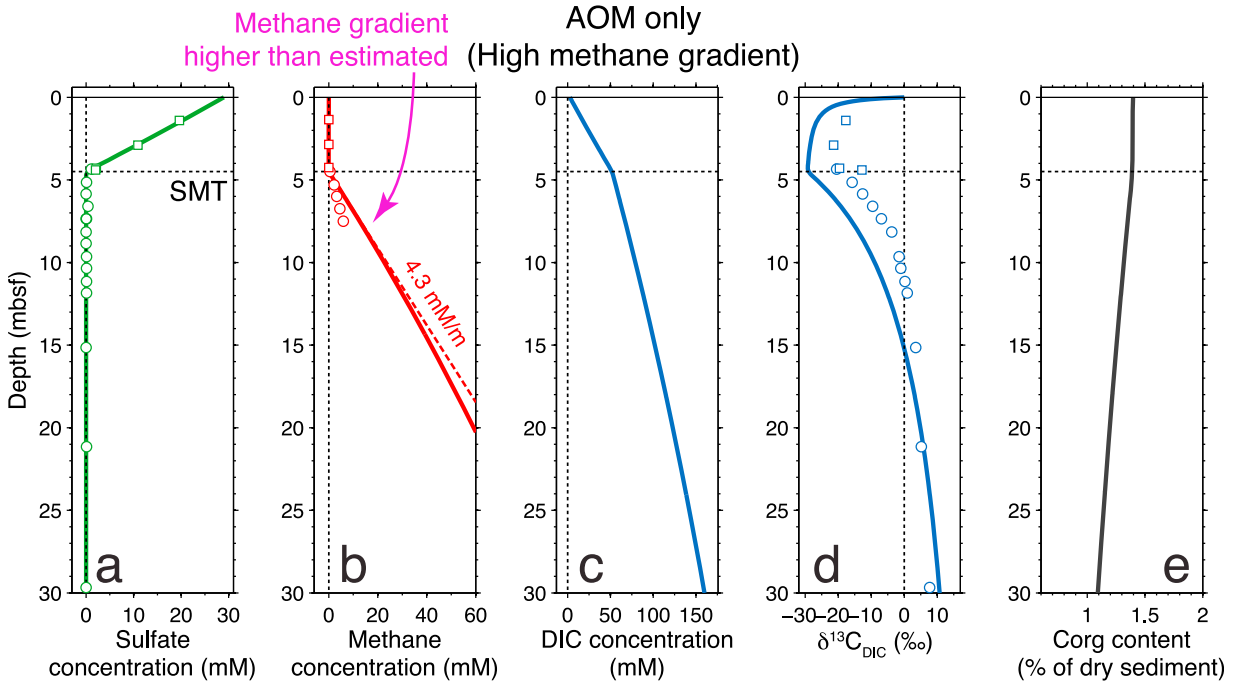


**Figure 8.** Modeled profiles of (a–c) solute concentrations, (d) $\delta^{13}$C-DIC, and (e) $C_{org}$ content if anaerobic oxidation of methane (AOM) is the only sulfate-consuming reaction at Site U1325. For AOM to consume all sulfate, the methane concentration gradient at the SMT must be 4.3 mM/m, which is almost twice the estimated methane gradient at Site U1325 (2.3 mM/m). Circles and squares in Figures 8a, 8b, and 8d are data from Hole U1325B and Hole U1325D, respectively (see Figure 2).

low (down to −65‰ [*Pohlman et al.*, 2008]). In these cases, the carbon isotopic signature is dominated by $^{13}$C-depleted methane carbon converted to DIC by AOM. Also, the DIC-sulfate ratio in the SRZ is close to 1:1 predicted for AOM in a closed system [*Kastner et al.*, 2008b] because no DIC enters the SRZ from below.

### 5.1.7. Methane Concentration Gradient

[50] As noted earlier, the 2.3 mM/m methane gradient at the SMT used here is conservatively low and could be higher. The highest possible value of the methane concentration gradient would be obtained if AOM was the only sulfate-consuming reaction, which means that the methane and sulfate flux at the SMT must match. The resulting maximum methane gradient computed for Site U1325 is 4.3 mM/m. The modeling results for this high value of the methane gradient (Figure 8) match the observations at Site U1325, with a minimum $\delta^{13}$C-DIC of −29.2‰, slightly more negative than that in the AOM-OSR combination scenario of Figure 6. Therefore, while we can definitely conclude that OSR cannot be the only sulfate reduction process, we cannot rule out AOM as the only sulfate reduction process at Site U1325.

[51] The main argument against AOM as the only sulfate reduction process is that the methane concentration gradient necessary for AOM to consume all the sulfate is almost twice the value we estimate at Site U1325. The pore water data and modeling results we use to estimate the methane gradient do not support such a large value. For example, the methane gradient estimated here is constrained by the actual depth to the top of the gas hydrate-bearing interval at Site U1325, where methane concentration reaches solubility [*Malinverno*, 2010]. A significantly steeper methane gradient at the SMT would imply a depth to the top of gas hydrate occurrence that is significantly shallower than that observed at Site U1325.

[52] On the other hand, the methane gradient could be somewhat greater than the 2.3 mM/m we estimate (e.g., due to pore water advection, which is not considered here). If the diffusive methane flux into the SMT were higher than our estimate, the sulfate sink due to AOM would increase and the sulfate sink due to OSR would decrease. Therefore, we conservatively estimate that at Site U1325 AOM consumes at least about half of the sulfate in the pore water.

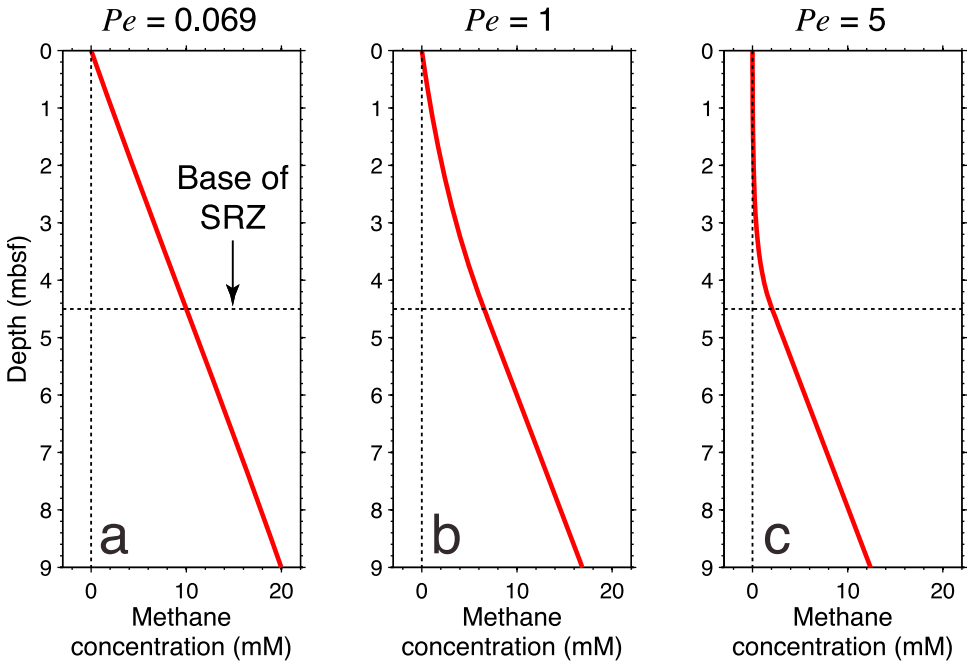


**Figure 9.** Calculated methane concentration profiles when sulfate is only consumed by OSR. (a) The sedimentation rate estimated at Site U1325 gives a Peclet number *Pe* in the SRZ that is well below 1, and methane diffuses into the SRZ. (b and c) Calculations for higher Peclet numbers show that a *Pe* of at least 5 is required for methane not to be present in the SRZ.

## 5.2. Do SMTs Require AOM?

[53] In the modeling results presented above, AOM must be active to reproduce the observation of no methane above the SMT at Site U1325. In this section we quantify the effect of different sedimentation rates and different SMT depths to determine if the widely observed absence of methane in the SRZ generally implies that AOM is active. This question is worth exploring because a high enough sedimentation rate could result in low methane concentrations in the SRZ even in the absence of the methane sink due to AOM [*Berner*, 1980].

[54] Consider the modeling scenario where OSR is the only sulfate-consuming reaction (Figure 5). Methane generated below the SRZ diffuses upward into the SRZ because there is no AOM to consume it at the SMT. The methane gradient at the seafloor is very close to the gradient at the base of the SRZ (Figure 5). Combining the methane concentration gradient at the seafloor $c_0'$ in equation (A4) with the methane source in equation (A8) and no fluid advection, we obtain a simple expression relating the methane gradient $c_0'$ at the seafloor to the gradient $c_{SMT}'$ at the SMT:

$$c_0' = c_{SMT}' \exp\left(-\frac{\omega z_{SMT}}{D}\right), \tag{6}$$

where $\omega$ is the sedimentation rate, $z_{SMT}$ the depth of the SMT, and $D$ the diffusion coefficient of methane in bulk sediment.

[55] The argument of the exponential in equation (6) is a dimensionless Peclet number, which quantifies the relative importance of diffusion and burial by sedimentation at a rate $\omega$ in a layer of thickness $z_{SMT}$ [*Boudreau*, 1997; *Bhatnagar et al.*, 2007]:

$$Pe = \frac{\omega z_{SMT}}{D}. \tag{7}$$

If $Pe > 1$, burial is more important than diffusion, whereas if $Pe < 1$ diffusion dominates over burial. If the rate of pore fluid burial (measured by the sedimentation rate) is high enough, it will overcome diffusion, resulting in little or no methane in the SRZ [*Berner*, 1980]. This is immediately shown by equation (6): a sedimentation rate $\omega$ that is large compared to $D/z_{SMT}$ results in a high *Pe* and a methane gradient at the seafloor approaching zero, meaning little or no methane in the SRZ. Conversely, a low sedimentation rate results in a small *Pe*, a methane gradient at the seafloor close to that at the base of the SRZ, and hence methane present in the SRZ.

[56] To determine the sedimentation rate needed to reproduce the observed lack of methane in the SRZ

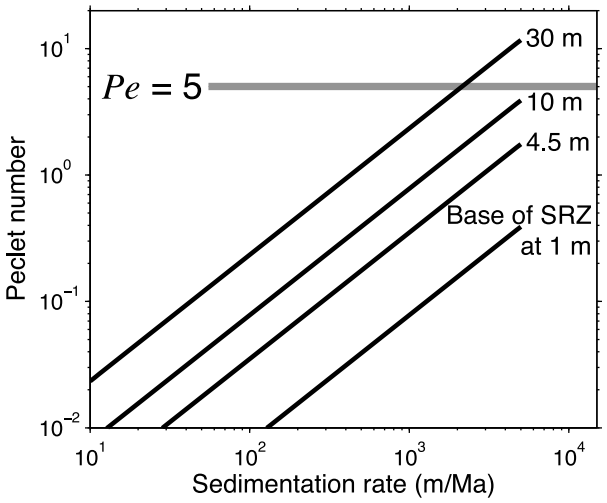


**Figure 10.** Peclet numbers in the SRZ versus sedimentation rate for different SRZ thicknesses. A Peclet number of 5, the minimum required to preclude methane from the SRZ in the absence of AOM (Figure 9), is only attained for thick SRZs (>30 m) and very high sedimentation rates (>2 km/Ma). In all other circumstances, methane will leak into the SRZ unless there is a methane sink at the SMT such as that provided by AOM.

without AOM, Figure 9 shows methane concentration profiles modeled for different Peclet numbers when OSR is the only sulfate-consuming reaction. The Site U1325 sedimentation rate and SMT depth (Table 2) give a $Pe = 0.069$, meaning that diffusion dominates over burial and methane leaks into the SRZ (Figure 9a). The case of $Pe = 1$ in Figure 9b is computed by artificially increasing the sedimentation rate. If $Pe = 1$, diffusion and burial are both important; the concentration of methane in the SRZ decreases somewhat, but it is still well above zero. To get a methane profile approaching that observed at Site U1325 without active AOM, the Peclet number must be raised to at least 5 (Figure 9c), which requires an unrealistic sedimentation rate that is more than seventy times that estimated at Site U1325.

[57] As the Peclet number is a dimensionless quantity that depends both on the depth of the SMT and the sedimentation rate, the results of Figure 9 can be extended to a range of SMT depths and sedimentation rates (Figure 10). For the SMT depths (1–30 m) and sedimentation rates (10–1000 m/Ma [*Seibold and Berger*, 1996]) typically observed in continental slope sediments, the Peclet number is always well below 5. If the Peclet number is less than 5, without AOM there will always be measurable amounts of methane in the SRZ and no well-defined SMT (Figure 9). Unless the base of the SRZ is very deep (>30 m) and the sedimentation rate extremely high (>2 km/Ma), the observation of a SMT with no methane above requires a sink of methane at the SMT such as that provided by AOM.

[58] These results imply that AOM must be active in continental margin sediments wherever there is a well-defined SMT, but do not require that AOM is the dominant sulfate-consuming reaction. It will be only when the upward flux of methane balances the downward flux of sulfate [*Borowski et al.*, 1996; *Niewöhner et al.*, 1998]. Also, the observation of a linear sulfate gradient from the seafloor to the SMT does not by itself imply that AOM is the dominant sulfate reduction process, as proposed by *Borowski et al.* [1996]. The results for the scenario where AOM and OSR consume an equivalent fraction of sulfate (Figure 6) show a nearly linear sulfate profile in the SRZ.

## 6. Conclusions

[59] Sulfate reduction processes consume methane and complex organic matter in shallow sediments within gas hydrate-bearing continental margins. Knowing the fraction of sulfate that serves as the terminal electron acceptor for either the anaerobic oxidation of methane (AOM) or organoclastic sulfate reduction (OSR) is important for estimating how much methane may be consumed by AOM and establishing whether sulfate gradients may be indicators of gas hydrate in the underlying sedimentary system.

[60] We developed a diagenetic model to determine if AOM is required to match the observed methane, sulfate, and dissolved inorganic carbon (DIC) profiles from IODP Expedition 311 Site U1325. The model demonstrates that first-order observations of no significant amounts of methane above the sulfate-methane transition (SMT) and a $\delta^{13}$C-DIC minimum at the SMT require that AOM consumes at least half of the sulfate. The $^{13}$C-enriched DIC values at the SMT and DIC-sulfate ratios similar to those expected from OSR are explained by upward diffusion of DIC produced by organic matter degradation and isotopically enriched with $^{13}$C by methanogenesis. We generalize these results beyond IODP Site U1325 with a dimensional analysis that accounts for the range of SMT depths (0–30 mbsf) and sedimentation rates (up to 2 km/Ma) typical of continental margins globally. We conclude that

AOM must be active in continental margin sediments wherever there are no significant quantities of methane above the SMT and the $\delta^{13}$C-DIC minimum is centered at the SMT, regardless of the absolute $\delta^{13}$C-DIC values or DIC-sulfate ratios.

# Appendix A: Solution of the Steady State Diagenetic Equation

[61] Assuming steady state conditions and constant porosity, the mass balance diagenetic equation (3) can be written as an ordinary differential equation with constant coefficients

$$D\frac{d^2c}{dz^2} - v\frac{dc}{dz} + \sum_{i=1}^{N} Q_i(z) = 0, \qquad \text{(A1)}$$

where $c$ is the desired solute concentration (moles per unit volume of pore fluid), $D$ is the diffusion coefficient in bulk sediment, $v$ is the vertical velocity of the pore fluid, and the $N$ reaction terms $Q_i$ (moles per unit volume of bulk sediment per unit time) define sources and sinks for the solute. The diffusion coefficient in bulk sediment is computed for each solute from the diffusion coefficient in water at 5°C [*Schulz*, 2006] divided by a tortuosity of 2.07, obtained from Archie's relationship [*McDuff and Ellis*, 1979] for a porosity $\phi = 0.65$ and coefficients estimated at Site U1325 [*Malinverno et al.*, 2008]. DIC in marine sediments is predominantly in the form of the bicarbonate ion [*Claypool et al.*, 2006], and we use the diffusion coefficient of bicarbonate for DIC.

## A1. Reaction Terms

[62] The reaction terms are defined as exponential functions limited to a finite depth interval:

$$Q_i(z) = \begin{cases} q_i \exp\left[-\dfrac{\lambda_i}{\omega}(z - a_i)\right], & a_i \le z \le b_i, \\ 0 & \text{elsewhere.} \end{cases} \qquad \text{(A2)}$$

where $q_i$ (positive for sources and negative for sinks) is the reaction rate at $z = a_i$, $\lambda_i$ is a reaction rate constant, and $\omega$ is the sedimentation rate. The reaction terms in equation (A2) allow for constant source/sink rates over a finite depth interval by letting $\lambda_i = 0$, or exponentially decaying sources/sinks that can have $b_i \to \infty$ (which requires $\lambda_i > 0$ to keep the source/sink finite). We define below the specific reaction terms for the different solutes, using an index $i = 1$ for sources/sinks due to OSR (reaction (2)), $i = 2$ for AOM (reaction (1)), and $i = 3$ for organic matter degradation (reaction (4)).

### A1.1. Sulfate

[63] There are two possible sinks for sulfate, due to AOM and to OSR. Writing the depth of the SMT as $z_{SMT}$ and its assumed thickness as $h_{SMT}$, the sulfate sink due to OSR is as in (A2) with $a_1 = 0$ and $b_1 = z_{SMT} - h_{SMT}/2$. In the case where OSR is the only sulfate-consuming reaction, the consumption rate $q_1$ that consumes all sulfate can be obtained by equating to zero the sulfate concentration in the solution (equation (A7)) for $z > z_{SMT}$.

[64] The AOM sulfate sink is as in equation (A2) with $a_2 = z_{SMT} - h_{SMT}/2$ and $b_2 = z_{SMT} + h_{SMT}/2$. The consumption rate due to AOM is assumed to be constant in depth (i.e., $\lambda_2 = 0$) and to match the diffusive methane flux into the SMT due to a methane concentration gradient $c'_{SMT}$. Equating this flux to the sink rate gives

$$q_2 = -\frac{D\,c'_{SMT}}{h_{SMT}}. \qquad \text{(A3)}$$

### A1.2. Methane

[65] There is a possible sink for sulfate due to AOM at the SMT and a source from organic matter degradation below the SMT. The AOM methane sink is identical to that of the AOM sulfate sink described above. The methane source is as in equation (A2) with $a_3 = z_{SMT} + h_{SMT}/2$ and $b_3 \to \infty$. The reaction time constant $\lambda_3$ has the value listed in Table 2, and the reaction rate $q_3$ at $z = a_3$ that gives rise to a methane concentration gradient $c'_{SMT}$ at the SMT is

$$q_3 = \left(\frac{D\lambda_3}{\omega} + v\right) c'_{SMT}. \qquad \text{(A4)}$$

### A1.3. DIC

[66] There are three possible sources for DIC, due to OSR, AOM, and organic matter degradation. As noted in the text, the DIC source due to OSR is minus twice the OSR sulfate sink, the DIC source due to AOM is minus the AOM sulfate sink, and the DIC source from organic matter degradation is the same as the corresponding methane source.

[67] To compute a $\delta^{13}$C-DIC profile, two separate solutions are obtained for DIC containing $^{12}$C and

$^{13}$C. The reaction rates $q_i$ are adjusted for the $\delta^{13}$C values of the respective sources. If the overall reaction rate is $q_i$, the reaction rates for $^{12}$C and $^{13}$C are

$$ {}^{12}q_i = q_i \frac{1}{1+R_i} \quad \text{and} \quad {}^{13}q_i = q_i \frac{R_i}{1+R_i}, \tag{A5} $$

where the $^{13}$C/$^{12}$C ratio $R_i$ is

$$ R_i = R_{\mathrm{PDB}}\left(1 + 0.001\,\delta^{13}\mathrm{C}_i\right), \tag{A6} $$

and

$$ P_i(z) = \begin{cases} 0 & z < a_i \\ S_i(z-a_i) & a_i \le z \le b_i, \\ S_i(z-a_i) - \exp\left[-\dfrac{\lambda_i}{\omega}(b_i-a_i)\right] S_i(z-b_i) & z > b_i, \end{cases} \tag{A9} $$

where

$$ S_i(x) = \begin{cases} \dfrac{D}{\lambda_i D + \omega v}\left[\exp\left(\dfrac{v}{D}x\right) - \exp\left(-\dfrac{\lambda_i}{\omega}x\right)\right] - \dfrac{1}{\lambda_i}\left[1 - \exp\left(-\dfrac{\lambda_i}{\omega}x\right)\right] & \lambda_i > 0, \\ \dfrac{D}{\lambda_i D + \omega v}\left[\exp\left(\dfrac{v}{D}x\right) - 1\right] + \dfrac{x}{\omega} & \lambda_i = 0. \end{cases} \tag{A10} $$

$\delta^{13}C_i$ is the $\delta^{13}$C of the $i$th DIC source, and $R_{\mathrm{PDB}}$ = 0.0112372 is the $^{13}$C/$^{12}$C ratio of the Pee Dee Belemnite standard.

## A2. Solution

[68] Solving equation (A1) requires two boundary conditions on the concentrations. At $z$ = 0, the concentrations are set to values $c_0$ that are typical ocean water values (29 mM for sulfate, 0 mM for methane, and 2.5 mM for DIC). The concentration at $z$ = 0 for DIC containing $^{12}$C and $^{13}$C is determined as done for the DIC sources, assuming that ocean water has a $\delta^{13}$C-DIC = 0. As all sources and sinks go to zero at great depth, the second boundary condition is a zero concentration gradient at $z \to \infty$.

[69] We solve equation (A1) with a Laplace transform method, which is well suited to reaction terms $Q_i$ that are restricted to finite depth intervals as in equation (A2). The solution is

$$ c(z) = c_0 + \frac{D}{v}\left[\exp\left(\frac{v}{D}z\right) - 1\right]c_0' - \frac{\omega}{v}\sum_{i=1}^{N} q_i P_i(z), \tag{A7} $$

where the concentration gradient at $z$ = 0 is

$$ c_0' = \sum_{i=1}^{N} \frac{q_i \omega}{\lambda_i D + \omega v} \cdot \left\{\exp\left[-\frac{v}{D}a_i\right] - \exp\left[-\frac{\lambda_i}{\omega}(b_i - a_i)\right]\exp\left[-\frac{v}{D}b_i\right]\right\} \tag{A8} $$

[70] In most of the solutions discussed in this paper, we assume constant porosity, no compaction and no active fluid advection. In this case, the fluid velocity $v$ equals the sedimentation rate $\omega$ in the equations above.

## Acknowledgments

[71] This research used samples and data provided by the Integrated Ocean Drilling Program (IODP). The efforts of the JOIDES Resolution shipboard and drilling personnel and of the scientific party of IODP Expedition 311 are gratefully acknowledged. We thank two anonymous reviewers for suggestions that improved the paper. This is L-DEO contribution 7477.

## References

Akiba, F., Y. Inoue, M. Saito-Kato, and J. W. Pohlman (2009), Data report: Diatom and foraminiferal assemblages in Pleistocene turbidite sediments from the Cascadia margin (IODP Expedition 311), northeast Pacific [online], *Proc. Integrated Ocean Drill. Program*, *311*, 22 pp., doi:10.2204/iodp.proc.311.211.2009. [Available at http://publications.iodp.org/proceedings/311/211/211_.htm]

Bekins, B. A., and S. J. Dreiss (1992), A simplified analysis of parameters controlling dewatering in accretionary prisms, *Earth Planet. Sci. Lett.*, *109*, 275–287.

Berner, R. A. (1980), *Early Diagenesis: A Theoretical Approach*, Princeton Univ. Press, Princeton, N. J.

Bhatnagar, G., W. G. Chapman, G. R. Dickens, B. Dugan, and G. J. Hirasaki (2007), Generalization of gas hydrate distribution and saturation in marine sediments by scaling of thermodynamic and transport processes, *Am. J. Sci.*, *307*, 861–900.

Blair, N. E., G. R. Plaia, S. E. Boehme, D. J. DeMaster, and L. A. Levin (1994), The remineralization of organic carbon on the North Carolina continental slope, *Deep Sea Res., Part II*, *41*, 755–766.

Borowski, W. S., C. K. Paull, and W. Ussler III (1996), Marine pore-water sulfate profiles indicate in situ methane flux from underlying gas hydrate, *Geology*, *24*, 655–658.

Borowski, W. S., T. M. Hoehler, M. J. Alperin, N. M. Rodriguez, and C. K. Paull (2000), Significance of anaerobic methane oxidation in methane-rich sediments overlying the Blake Ridge gas hydrates, *Proc. Ocean Drill. Program Sci. Results*, *164*, 87–99.

Boudreau, B. P. (1997), *Diagenetic Models and Their Implementation*, Springer, Berlin.

Burns, S. J. (1998), Carbon isotopic evidence for coupled sulfate reduction-methane oxidation in Amazon Fan sediments, *Geochim. Cosmochim. Acta*, *62*, 797–804.

Chatterjee, S., G. Bhatnagar, W. G. Chapman, G. R. Dickens, B. Dugan, and G. J. Hirasaki (2009), Sulfate, methane, alkalinity, calcium and carbon isotope ($\delta^{13}C$) profiles as an indicator of upward methane flux, *Eos Trans. AGU*, *90*(52), Fall Meet. Suppl., Abstract OS42A-05.

Claypool, G. E., and I. R. Kaplan (1974), The origin and distribution of methane in marine sediments, in *Natural Gases in Marine Sediments*, edited by I. R. Kaplan, pp. 99–139, Plenum, New York.

Claypool, G. E., and C. N. Threlkeld (1983), Anoxic diagenesis and methane generation in sediments of the Blake Outer Ridge, Deep Sea Drilling Project Site 533, Leg 76, *Initial Rep. Deep Sea Drill. Proj.*, *76*, 391–402.

Claypool, G. E., A. V. Milkov, Y.-J. Lee, M. E. Torres, W. S. Borowski, and H. Tomaru (2006), Microbial methane generation and gas transport in shallow sediments of an accretionary complex, southern Hydrate Ridge (ODP Leg 204), offshore Oregon, USA, *Proc. Ocean Drill. Program Sci. Results*, *204*, 1–52.

Colwell, F. S., S. Boyd, M. E. Delwiche, D. W. Reed, T. J. Phelps, and D. T. Newby (2008), Estimates of biogenic methane production rates in deep marine sediments at Hydrate Ridge, Cascadia Margin, *Appl. Environ. Microbiol.*, *74*, 3444–3452, doi:10.1128/AEM.02114-07.

Davie, M. K., and B. A. Buffett (2001), A numerical model for the formation of gas hydrate below the seafloor, *J. Geophys. Res.*, *106*, 497–514.

Davie, M. K., O. Y. Zatsepina, and B. A. Buffett (2004), Methane solubility in marine hydrate environments, *Mar. Geol.*, *203*, 177–184.

Dickens, G. R., and G. T. Snyder (2009), Interpreting upward methane flux from marine pore water profiles, in *Fire in the Ice*, winter, pp. 7–10, Natl. Energy Technol. Lab., U.S. Dep. of Energy, Washington, D. C.

Heuer, V. B., J. W. Pohlman, M. E. Torres, M. Elvert, and K.-U. Hinrichs (2009), The stable carbon isotope biogeochemistry of acetate and other dissolved carbon species in deep subseafloor sediments at the northern Cascadia Margin, *Geochim. Cosmochim. Acta*, *73*, 3323–3336, doi:10.1016/j.gca.2009.03.001.

Hinrichs, K.-U., and A. Boetius (2002), The anaerobic oxidation of methane: New insights in microbial ecology and biogeochemistry, in *Ocean Margin Systems*, edited by G. Wefer et al., pp. 457–477, Springer, Berlin.

Hoehler, T. M., M. J. Alperin, D. B. Albert, and C. S. Martens (1994), Field and laboratory studies of methane oxidation in an anoxic marine sediment: Evidence for a methanogen-sulfate reducer consortium, *Global Biogeochem. Cycles*, *8*, 451–463.

Ingall, E. D., and P. Van Cappellen (1990), Relation between sedimentation rate and burial of organic phosphorus and organic carbon in marine sediments, *Geochim. Cosmochim. Acta*, *54*, 373–386.

Jørgensen, B. B., A. Weber, and J. Zopfli (2001), Sulfate reduction and anaerobic methane oxidation in Black Sea sediments, *Deep Sea Res., Part I*, *48*, 2097–2120.

Kastner, M., M. E. Torres, E. A. Solomon, and A. J. Spivack (2008a), Marine pore fluid profiles of dissolved sulfate: Do they reflect in situ methane fluxes?, in *Fire in the Ice*, summer, pp. 6–8, Natl. Energy Technol. Lab., U.S. Dep. of Energy, Washington, D. C.

Kastner, M., G. E. Claypool, and G. Robertson (2008b), Geochemical constraints on the origin of the pore fluids and gas hydrate distribution at Atwater Valley and Keathley Canyon, northern Gulf of Mexico, *Mar. Pet. Geol.*, *25*, 860–872, doi:10.1016/j.marpetgeo.2008.01.022.

Kim, J.-H., and Y.-J. Lee (2009), Data report: Elemental, Rock-Eval, and isotopic compositions of bulk sediments, IODP Expedition 311 [online], *Proc. Integrated Ocean Drill. Program*, *311*, 15 pp. [Available at http://publications.iodp.org/proceedings/311/ERR/CHAPTERS/311_207.PDF]

Malinverno, A. (2010), Marine gas hydrates in thin sand layers that soak up biogenic methane, *Earth Planet. Sci. Lett.*, *292*, 399–408, doi:10.1016/j.epsl.2010.02.008.

Malinverno, A., M. Kastner, M. E. Torres, and U. G. Wortmann (2008), Gas hydrate occurrence from pore water chlorinity and downhole logs in a transect across the northern Cascadia margin (Integrated Ocean Drilling Program Expedition 311), *J. Geophys. Res.*, *113*, B08103, doi:10.1029/2008JB005702.

McCorkle, D. C., and S. R. Emerson (1988), The relationship between pore water carbon isotopic composition and bottom water oxygen concentration, *Geochim. Cosmochim. Acta*, *52*, 1169–1178.

McDuff, R. E., and R. A. Ellis (1979), Determining diffusion coefficients in marine sediments: A laboratory study of the validity of resistivity techniques, *Am. J. Sci.*, *279*, 666–675.

Milkov, A. V., and R. Sassen (2002), Economic geology of offshore gas hydrate accumulations and provinces, *Mar. Pet. Geol.*, *19*, 1–11.

Moore, T. S., R. W. Murray, A. C. Kurtz, and D. P. Schrag (2004), Anaerobic methane oxidation and the formation of dolomite, *Earth Planet. Sci. Lett.*, *229*, 141–154, doi:10.1016/j.epsl.2004.10.015.

Niewöhner, C., C. Hensen, S. Kasten, M. Zabel, and H. D. Schulz (1998), Deep sulfate reduction completely mediated by anaerobic methane oxidation in sediments of the upwelling area off Namibia, *Geochim. Cosmochim. Acta*, *62*, 455–464.

Paull, C. K., and W. Ussler III (2001), History and significance of gas sampling during DSDP and ODP drilling associated with gas hydrates, in *Natural Gas Hydrates: Occurrence, Distribution, and Detection*, *Geophys. Monogr. Ser.*, vol. 124, edited by C. K. Paull and W. P. Dillon, pp. 53–65, AGU, Washington, D. C.

Paull, C. K., W. Ussler III, T. D. Lorenson, W. J. Winters, and J. Dougherty (2005), Geochemical constraints on the distribution of gas hydrates in the Gulf of Mexico, *Geo Mar. Lett.*, *25*, 273–280, doi:10.1007/s00367-005-0001-3.

Pohlman, J. W., C. Ruppel, D. R. Hutchinson, R. Downer, and R. B. Coffin (2008), Assessing sulfate reduction and methane cycling in a high salinity pore water system in the northern Gulf of Mexico, *Mar. Pet. Geol.*, *25*, 942–951, doi:10.1016/j.marpetgeo.2008.01.016.

Pohlman, J. W., M. Kaneko, V. B. Heuer, R. B. Coffin, and M. Whiticar (2009), Methane sources and production in the

northern Cascadia margin gas hydrate system, *Earth Planet. Sci. Lett.*, *287*, 504–512, doi:10.1016/j.epsl.2009.08.037.

Presley, B. J., and I. R. Kaplan (1968), Changes in dissolved sulfate, calcium and carbonate from interstitial water of near-shore sediments, *Geochim. Cosmochim. Acta*, *32*, 1037–1048.

Reeburgh, W. S. (1976), Methane consumption in Cariaco Trench waters and sediments, *Earth Planet. Sci. Lett.*, *28*, 337–344.

Reeburgh, W. S. (2007), Oceanic methane biogeochemistry, *Chem. Rev.*, *107*, 486–513.

Riedel, M., T. S. Collett, M. J. Malone, and Expedition 311 Scientists (2006), *Proceedings of the Integrated Ocean Drilling Program*, vol. 311, Integrated Ocean Drill. Program, College Station, Tex., doi:10.2204/iodp.proc.311.2006.

Ruppel, C., G. R. Dickens, D. G. Castellini, W. Gilhooly, and D. Lizarralde (2005), Heat and salt inhibition of gas hydrate formation in the northern Gulf of Mexico, *Geophys. Res. Lett.*, *32*, L04605, doi:10.1029/2004GL021909.

Schulz, H. D. (2006), Quantification of early diagenesis: Dissolved constituents in pore water and signals in the solid phase, in *Marine Geochemistry*, edited by H. D. Schulz and M. Zabel, 2nd ed., pp. 73–124, Springer, Berlin.

Seibold, E., and W. H. Berger (1996), *The Sea Floor: An Introduction to Marine Geology*, 3rd ed., Springer, Berlin.

Sivan, O., D. P. Schrag, and R. W. Murray (2007), Rates of methanogenesis and methanotrophy in deep-sea sediments, *Geobiology*, *5*, 141–151, doi:10.1111/j.1472-4669.2007.00098.x.

Snyder, G. T., A. Hiruta, R. Matsumoto, G. R. Dickens, H. Tomaru, R. Takeuchi, J. Komatsubara, Y. Ishida, and H. Yu (2007), Pore water profiles and authigenic mineralization in shallow marine sediments above the methane-charged system on Umitaka Spur, Japan Sea, *Deep Sea Res., Part II*, *54*, 1216–1239, doi:10.1016/j.dsr2.2007.04.001.

Teichert, B. M. A., N. Gussone, A. Eisenhauer, and G. Bohrmann (2005), Clathrites: Archives of near-seafloor pore-fluid evolution ($\delta^{44/40}$Ca, $\delta^{13}$C, $\delta^{18}$O) in gas hydrate environments, *Geology*, *33*, 213–216.

Torres, M. E., and M. Kastner (2009), Data report: Clues about carbon cycling in methane-bearing sediments using stable isotopes of the dissolved inorganic carbon, IODP Expedition 311 [online], *Proc. Integrated Ocean Drill. Program*, *311*, 8 pp., doi:10.2204/iodp.proc.311.206.2009. [Available at http://publications.iodp.org/proceedings/311/ERR/CHAPTERS/311_206.PDF]

Torres, M. E., K. Wallmann, A. M. Tréhu, G. Bohrmann, W. S. Borowski, and H. Tomaru (2004), Gas hydrate growth, methane transport, and chloride enrichment at the southern summit of Hydrate Ridge, Cascadia margin off Oregon, *Earth Planet. Sci. Lett.*, *226*, 225–241, doi:10.1016/j.epsl.2004.07.029.

Tréhu, A. M., C. Ruppel, M. Holland, G. R. Dickens, M. E. Torres, T. S. Collett, D. S. Goldberg, M. Riedel, and P. Schultheiss (2006), Gas hydrates in marine sediments: Lessons from scientific ocean drilling, *Oceanography*, *19*, 124–142.

Treude, T., J. Niggemann, J. Kallmeyer, P. Wintersteller, C. J. Schubert, A. Boetius, and B. B. Jørgensen (2005), Anaerobic oxidation of methane and sulfate reduction along the Chilean continental margin, *Geochim. Cosmochim. Acta*, *69*, 2767–2779, doi:10.1016/j.gca.2005.01.002.

Ussler, W., III, and C. K. Paull (2008), Rates of anaerobic oxidation of methane and authigenic carbonate mineralization in methane-rich deep-sea sediments inferred from models and geochemical profiles, *Earth Planet. Sci. Lett.*, *266*, 271–287, doi:10.1016/j.epsl.2007.10.056.

Whiticar, M. J. (1999), Carbon and hydrogen isotope systematics of bacterial formation and oxidation of methane, *Chem. Geol.*, *161*, 291–314.